

Pore Surface Functionalization of MCM-48 Mesoporous Silica with Tungsten and Molybdenum Metal Centers: Perspectives on Catalytic Peroxide Activation

M. S. Morey,[†] J. D. Bryan,[†] S. Schwarz,[‡] and G. D. Stucky^{*,†}

Chemistry Department, University of California, Santa Barbara, California 93106, and DuPont Experimental Station, Wilmington, Delaware 19880-0262

Received January 27, 2000. Revised Manuscript Received August 14, 2000

The pore surface of MCM-48 mesoporous silica was functionalized with tungsten and molybdenum metal centers by the anhydrous reaction of metal alkoxides with surface silanol groups. Resulting metal–oxo species were attached via covalent M–O–Si bonds as confirmed with photoacoustic (PAS)-FTIR. Diffuse reflectance UV–visible spectroscopy indicates that the metal oxo groups are predominantly comprised of tetrahedral and octahedral coordinated monomers. MCM-48 grafted with Mo and W is active for brominating phenol red with hydrogen peroxide at neutral pH in a manner similar to Ti–MCM-48, as we reported earlier. The rates of bromination for Mo, W, and four other metals, after normalization for metal concentration, measured as absorption peak intensities of the resultant bromophenol blue, are as follows: 50:46:16:2.8:1:0 W:Mo:Ti:Zr:V:Re. The different rates of reactivity, and hence the general degree of metal–peroxo activation, can be explained on the basis of size, charge, coordination sphere, and electronegativity of the central metal.

Introduction

Silica and alumina substrates have been used for decades to support transition metal oxides for catalytic applications. These supports are attractive for their high specific surface area, mechanical stability, and promotion of well-dispersed active metal sites. With the advent of mesoporous silica by a Japanese group and later by Mobil scientists,¹ a new avenue for catalysis was paved. Formed through a cooperative self-assembly process of oligomeric silicate anions and amphiphilic surfactant molecules,² mesoporous silicates provide an ordered array of accessible pore volumes for surface modification and application based chemistry. The silicate oligomers assume the minimal surface morphology between the headgroups of the surfactant micelles in the self-assembled liquid crystal system. Of the many possible mesoporous silica materials, we chose the cubic MCM-48 phase for its three-dimensional pore array enabling reactive species access along all three crystallographic directions. This choice becomes crucial when considering pore orientation effects in thin film membrane applications, for example.³

We have previously used mesoporous silica to support isolated vanadium,^{4,5} zirconium,⁶ and titanium metal

centers.^{7,8} In each case, a water-sensitive metal alkoxide was reacted with surface silanols within the pores to generate isolated metal centers for catalytic applications. Isolated titanium centers grafted on mesoporous silica in this manner have been found to catalyze the halogenation of large organic substrates facilitated by the high surface area and pore diameters of the support.⁹ This behavior is closely analogous to the role of the vanadium peroxidase (V–BrPO) enzyme which performs this function in the marine environment to produce brominated natural products with pharmacological activity, possibly preventing the host organism from being infected or eaten.^{10–12} Although there are a number of transition metal-containing V–BrPO mimics, this grafted material is the first active catalyst reported that functions at neutral pH. By using a halide salt and hydrogen peroxide, these materials provide an alternative to corrosive and toxic metal chlorides or bromine for halogenation and thus warrant further study.¹³

In an attempt to improve upon the activity of the heterogeneous catalyst Ti/MCM-48, three additional

(5) VanDerVoort, P.; Morey, M. S.; Stucky, G. D.; Mathieu, M.; Vansant, E. F. *J. Phys. Chem. B* **1998**, *102*, 585.

(6) Morey, M. S.; Schwarz, S.; Fröba, M.; Stucky, G. D. *J. Phys. Chem. B* **1999**, *103*, 2037.

(7) Morey, M. S.; Davidson, A.; Stucky, G. *Microporous Mater.* **1996**, *6*, 99.

(8) Morey, M. S.; O'Brien, S.; Schwarz, S.; Stucky, G. D. *Chem. Mater.* **2000**, *12*, 898.

(9) Walker, J. V.; Morey, M. S.; Carlsson, H.; Davidson, A.; Stucky, G. D.; Butler, A. *J. Am. Chem. Soc.* **1997**, *119*, 6921.

(10) Butler, A.; Walker, J. V. *Chem. Rev.* **1993**, *93*, 1937. Meister, G.; Butler, A. *Inorg. Chem.* **1994**, *33*, 3269.

(11) Clague, M.; Butler, A. *J. Am. Chem. Soc.* **1995**, *117*, 3475.

(12) Colpas, G. J.; Hamstra, B. J.; Kampf, J. W.; Pecoraro, V. L. *J. Am. Chem. Soc.* **1996**, *118*, 3469.

(13) Morey, M. S. Ph.D. Dissertation, University of California, Santa Barbara, CA, 1998.

[†] University of California.

[‡] DuPont Experimental Station.

(1) (a) Yanagisawa, T.; Shimizu, T.; Kuroda, K.; Kato, D. *Bull. Chem. Soc. Jpn.* **1990**, *63*, 988. (b) Kresge, C. T.; Leonowicz, M. E.; Roth, W. J.; Vartuli, J. C.; Beck, J. S. *Nature* **1992**, *359*, 710.

(2) Monnier, A.; Schüth, F.; Huo, Q.; Kumar, D.; Margolese, D.; Maxwell, R. S.; Stucky, G. D.; Krishnamurty, M.; Petroff, P.; Firouzi, A.; Janicke, M.; Chmelka, B. F. *Science* **1993**, *261*, 1299.

(3) Nishiyama, N.; Koide, A.; Egashira, Y.; Ueyama, K. *Chem. Commun.* **1998**, 2147.

(4) Morey, M. S.; Davidson, A.; Eckert, H.; Stucky, G. *Chem. Mater.* **1996**, *8*, 486.

transition metals (Mo, Re, W) were similarly assessed for halogenating ability on the basis of the known halogenating activity of their oxyanions and their ability to coordinate peroxide ligands. Molybdenum and tungsten, for example, are known to form anions containing up to four peroxy ligands.¹⁴ Mo- and W-incorporated MCM-41 has also been found to be quite active for oxidative catalytic conversions and hydrocracking of hydrocarbons.^{15–19} Likewise, methyltrioxorhenium has been found to be very active for homogeneous catalytic epoxidation reactions.^{20,21} Spanning all three rows of the d-block elements, these metal atoms vary in size, formal charge, and electronegativity and result in a wide range of reactivity rates. As with titanium, it is believed that, in order to oxidize bromide, the formation of a reactive metal peroxide intermediate is required. Once coordinated, the central metal must then facilitate the cleavage of the O–O bond for a useful reaction to occur. Using electronic and vibrational spectroscopic methods we first characterize the nature of the surface species and their interaction with the hydrogen peroxide molecule. This information combined with preliminary catalysis results will be used to comment on the comparative reactivity of each supported metal and on general tendencies of peroxide activation by immobilized transition metal complexes.

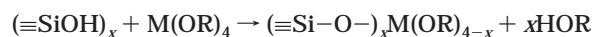
Experimental Section

Reagent grade tetraethyl orthosilicate (TEOS) was provided by Fisher, and cetylbenzyltrimethylammonium chloride (CB-DAC) was from Kodak. Rhenium(III) chloride was purchased from Aldrich. Tungsten(V) ethoxide (W(OEt)₅, 95%), molybdenum(V) ethoxide (Mo₂(OEt)₁₀ with small impurity of MoO(OEt)₃, 90%), vanadium(V) oxide triisopropoxide (O=V(iOPr)₃), zirconium propoxide (Zr(OPr)₄), and titanium isopropoxide (Ti(iOPr)₄) were purchased from Gelest. All chemicals were used as received.

For a pure silica, cubic mesopore (denoted MCM-48 or blank), 7.88 g (19 mmol) of CBDAC was dissolved in 171 g (9.5 mol) of deionized water with heating. The surfactant CBDAC was chosen because it was found to favor the MCM-48 mesophase. The pH was raised to ~12 with 10 g (20 mmol) of 2 M (TMA)OH followed by 10.42 g (50 mmol) of TEOS. This solution was rapidly stirred for 2 h and then transferred to a 500 mL Teflon bottle and placed in a 100 °C oven for 15 days. The product was filtered and then returned to the 100 °C oven for an additional 8 days to give a more crystalline product as determined by X-ray powder diffraction. The final product was filtered out, washed with water followed by methanol, and then calcined at 550 °C for 6 h in nitrogen and then air to remove the surfactant. The yield was approximately 80% based on TEOS (Si).

Tungsten, titanium, zirconium, and vanadium were grafted in a similar manner as described previously.^{4,6,8} Metal-grafted samples were made by first dehydrating a calcined sample of pure silica MCM-48 at 200 °C under a rough vacuum over-

night. In an argon-purged glovebag, the support was then mixed with the metal alkoxide/hexane solution, at the desired concentration from 2 to 12 mol % and reacted according to the following equation:



To graft molybdenum, the solid ethoxide was dissolved in ethanol to give a 0.21 M solution and then combined with the dehydrated support to give a 5 mol % Mo content in the final product. In the case of tungsten, liquid W(OEt)₅ was used directly with hexane to make a 7.4 mol % W on MCM-48, referred to as (XS-W). After reacting for 2 h, the products were filtered off and washed with hexane and then calcined at 400 °C under flowing O₂ in a tube furnace for 4 h to remove residual organics and convert ≡SiO–M(OR)_n groups to ≡SiO–M(OH)_n groups.

Rhenium was coated on the silica surface by mixing a less-rigorously dehydrated sample of MCM-48 with a saturated ReCl₃/ethanol solution. The slurry was sonicated for a few minutes and then left to evaporate overnight. This process was repeated once again to generate a gray powder (total of 4.75 g of ReCl₃ solution added to 0.12 g of MCM-48). The sample was then calcined in flowing oxygen for 3 h at 350 °C yielding a white powder. A grafting blank was prepared by dehydrating a pure silica MCM-48 sample, soaking it in hexane, and then calcining at 400 °C for 4 h. This sample was analyzed by both XRD and PAS-FTIR described below.

X-ray powder diffraction patterns were obtained on a Scintag PADX diffractometer using Cu Kα radiation with a liquid-nitrogen-cooled solid-state detector at 45 kV and 40 mA. Nitrogen absorption/desorption isotherms were measured on a Micromeritics ASAP 2000 apparatus. All samples were outgassed initially at room temperature and then at 200 °C until a pressure <1 mTorr was achieved. Surface areas calculated by the Brunauer, Emmett, and Teller method for each material.²² Pore diameter distribution curves were calculated by the BJH (Barrett–Joyner–Halenda) method²³ using the Halsey equation for multilayer thickness and came from the analysis of the adsorption branch of the isotherm.

Scanning electron microscopy was performed on a JEOL JSM-6300F. An accelerating voltage of 3 kV was used at a magnification of 13 000×. Thin moderately uniform layers of the sample were placed onto carbon tape SEM disks and desiccated for 12 h to remove any water. A thin gold layer was deposited onto the sample in a metal-deposition chamber to ensure conductance of the sample and eliminate static charge buildup.

The UV/visible spectra were measured with a Cary 5 UV/vis-NIR spectrophotometer equipped with the Varian diffuse reflectance accessory. The halon/quartz cover slide that covers the sample was subtracted out of every scan. The Teflon integrating sphere that was used has very low absorbance in the range of our scans and hence has negligible influence on our results. Samples were run dry and in a slurry of water. The standard Kubelka Munk function was used to analyze the data.²⁴

The mid-infrared spectra have been collected on the Nicolet Magna 850 FT-IR spectrometer by the coaddition of 250 scans at a 4 cm⁻¹ resolution, using an MTEC model 300 photoacoustic detector in photoacoustic mode, ultrapure He as a gas vector (15 cm³/min), and a KBr sample window. Since the signal intensity is inversely proportional to the gas volume above the sample cup, care was taken to fill the sample cup flush with the rim each time. Each spectrum was divided by a carbon black reference standard. The photoacoustic detector allows pure samples to be run, avoiding KBr dilution errors and catastrophic structural collapse during pellet making that can occur in transmission mode analysis. Qualitative subtraction

(14) Dickman, M. H.; Pope, M. T. *Chem. Rev.* **1994**, *94*, 569.

(15) Corma, A.; Martinez, A.; Martinez-Soria, V.; Monton, J. B. *J. Catal.* **1995**, *153*, 25.

(16) Rana, R. K.; Viswanathan, B. *Catal. Lett.* **1998**, *52*, 25.

(17) Zhang, Z. R.; Suo, J. S.; Zhang, X. M.; Li, S. B. *Chem. Commun.* **1998**, 241.

(18) Ookoshi, T.; Onaka, M. *Chem. Commun.* **1998**, 2399.

(19) Piquemal, J.-Y.; Manoli, J.-M.; Beunier, P.; Ensueque, A.; Tougne, P.; Legrand, A.-P.; Bregeault, J.-M. *Microporous Mesoporous Mater.* **1999**, *29*, 291.

(20) Espenson, J. H.; Pestovsky, O.; Huston, P.; Staudt, S. *J. Am. Chem. Soc.* **1994**, *116*, 2869.

(21) Adam, W.; Mitchell, C. M.; Saha-Moller, C. R. *J. Org. Chem.* **1999**, *64*, 3699.

(22) Brunauer, S.; Emmett, P. H.; Teller, E. *J. Am. Chem. Soc.* **1938**, *60*, 309.

(23) Barrett, E. P.; Joyner, L. G.; Halenda, P. P. *J. Am. Chem. Soc.* **1951**, *73*, 373.

(24) Kubelka, P.; Munk, F. *Z. Tech. Phys.* **1931**, *12*, 593.

spectra were made from spectra with normalized intensities, with the blank being subtracted from each metal-containing sample. The sampling depth of the IR beam is assumed to be nearly identical between the pure silica and the grafted samples, due to the relatively low metal loadings.

Catalyst testing was performed in the same manner as previously reported.⁹ A total of 5–10 mg of the material was placed in a small test tube followed by a 1 mL solution of 5 mM phenol red, 0.1 M KBr, 50 mM H₂O₂, and 0.1 M HEPES buffer (pH 6.5). Each tube was shaken vigorously. At fixed time intervals, the tube was centrifuged and then a small aliquot was withdrawn and diluted. To establish that the materials were truly catalytic, a run with more moles of phenol red than grafted metal was performed. For this longer run, extra H₂O₂ had to be added to get the bromination to go to completion, since hydrogen peroxide is both participating in the reaction and slowly decomposing. The degree of bromination was determined by measuring the peak intensity of bromophenol blue (589 nm) with UV/vis in each aliquot. A blank, without catalyst, showed no activity toward bromination.

To determine the role aqueous metal ions play in the bromination reaction, the degree of metal leaching from the most active W, Mo, and Ti catalysts was determined. First, the three samples were treated at 400 °C and divided into 5 × 30 mg portions. Each was immersed in a 3 mL aliquot of the above solution followed by 40 min in an ultrasound bath and an additional 3 h under static conditions. The brutal ultrasound treatment was used to find the maximum metal that could be leached. Some breakdown of the support was noted in the formation of a fine silt which would likely have a profound effect on the amount of leaching. This test was repeated on the Ti and W samples after calcining them to 800 °C in static air for 4 h, without sonication. This is the maximum temperature MCM-48 can survive before catastrophic condensation of the pore system. Mo/MCM-48 was not tested since the melting point of MoO₃ is slightly below 800 °C and the nature of the surface species might change. As a rough test of the activity of the supernatant, a sample tube was prepared containing pure silica MCM-48 and a portion of either sodium salt of Mo or W corresponding in concentration to 100% leaching of a 5 at. % catalyst. Each tube was shaken and observed for color change.

Elemental analyses were performed by Galbraith Laboratories, Knoxville, TN.

Macroscopic Characterization of Metal-Grafted Materials

Following the grafting process, the main diffraction peaks that index to the MCM-48 mesophase in the *Ia3d* space group² are clearly visible by X-ray powder diffraction patterns (Figure 1). The support undergoes two additional heating steps, dehydration at 200 °C and calcination to oxidize the metal centers at 400 °C, which tends to cause a slight shrinkage of the pores and hence the unit cell. As with each metal grafted, no peaks are observed at higher angles due to metal oxide clusters. Peaks are still retained as a preliminary indication that there are still pore openings, even if slightly constricted. If the pores were filled, XRD peaks would be greatly attenuated since the difference in electron density between the silica walls and the metal oxide filling would be minimal. This effect would be analogous to the increase in peak intensity that occurs after removal of the surfactant template by calcination. In the case of the grafting blank, the diffractogram is essentially unchanged from the original support. All samples were found to have retained a high surface area and narrow pore distribution as determined by nitrogen sorption studies with the exception of the rhenium sample which was not tested. Surface areas averaged over 1000 m²/g

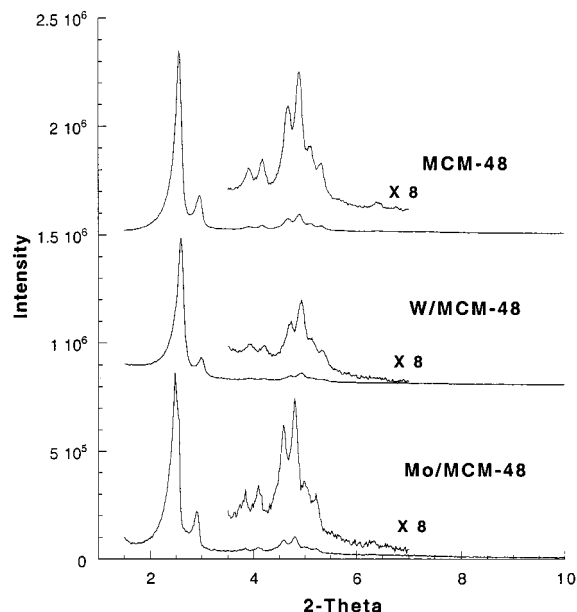


Figure 1. X-ray powder diffraction patterns of pure, calcined MCM-48, grafted with tungsten and molybdenum.

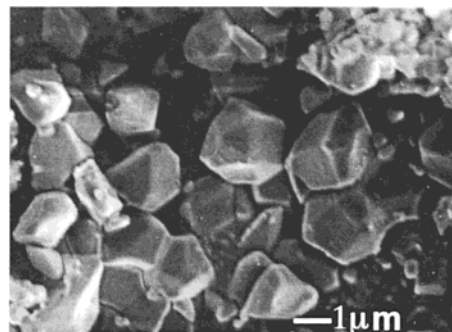


Figure 2. Scanning electron micrograph of pure silica MCM-48 single crystals.

and pore diameters ranged from 22 to 25 Å, which is sufficient to accommodate large organic substrates such as phenol red. SEM studies of the calcined, pure silica MCM-48 support show regions of single crystals in the 1–2 μm (Figure 2). These single crystals are similar to the rhomb dodecahedra resulting from truncated cubes reported by Ryoo et al.²⁵ For a powder composed of spheres with known density (ρ) and radius (r), the surface area (S) can be calculated with the following equation: $S = 3/(\rho r)$. Mesoporous silica has a density similar to amorphous silica of 2.2 g/cm³. Using the SEM particle size data and the above density, it can be shown that 99.9% of the surface area is due to the porous nature of these materials. This fact explains the ability of MCM-48 to uptake a relatively high mole percent of evenly distributed transition metal centers during grafting while showing little to no detectable formation of bulk metal oxide clusters.

Given the surface area and mole percent loading for supported metal, the coverage can be roughly calculated. For example, when tungsten is grafted, a maximum coverage of 7.4 mol % is achieved. The metal coverage in atoms/nm² can be calculated by assuming the metal atom layer thickness to be negligible and using an

(25) Kim, J. M.; Kim, S. K.; Ryoo, R. *Chem. Commun.* **1998**, 259.

Table 1. Calculated Grafted Metal Ion Coverages Using an Average, Fixed Surface Area of 1250 m²/g and Elemental Analysis Results^a

	tungsten	molybdenum	zirconium	titanium	vanadium
mol %	7.4	2.1	11.9	17.5	18.3
atoms/ nm ²	0.37	0.15	0.66	1.00	1.04

^a Rhenium was found to be inactive for bromination, so it was only characterized by PAS-FTIR

average support surface area of 1250 m²/g. For comparison, the approximate abundance of surface silanols on calcined MCM-48 is between 1.4 and 1.8/nm².⁵⁶ The maximum coverage that can be attained for each metal on calcined MCM-48 using a stoichiometric excess of metal alkoxide is given in Table 1. The trends seen for metal ion coverage using the metal alkoxide route are most easily described by the reactivity of the precursor. While vanadium and titanium alkoxides are very water sensitive, molybdenum ethoxide is a relatively stable solid, sparingly soluble in ethanol.

Leaching studies show that the surface interaction between the silica and the most active grafted metals (Ti, Mo, W) is moderately robust. When samples were submitted to rigorous sonication in a solution identical to the catalytic tests, we found the following average amount of metal leaching: Ti, 8.6%; Mo, 49.1%; W, 22.4%. These conditions far exceeded the more benign conditions used in the actual catalytic test but were used to find the maximum leaching levels. While the concentrations are quite high, much of the dissolution is the result of fragmentation of the silica support and the local heating of the supernatant. In an attempt to make the materials more suitable for reuse after a reaction, each was heated to 800 °C for 4 h and tested again. This time, the amount of leaching was reduced significantly and is as follows: Ti, 0.88%; W, 9.0%.

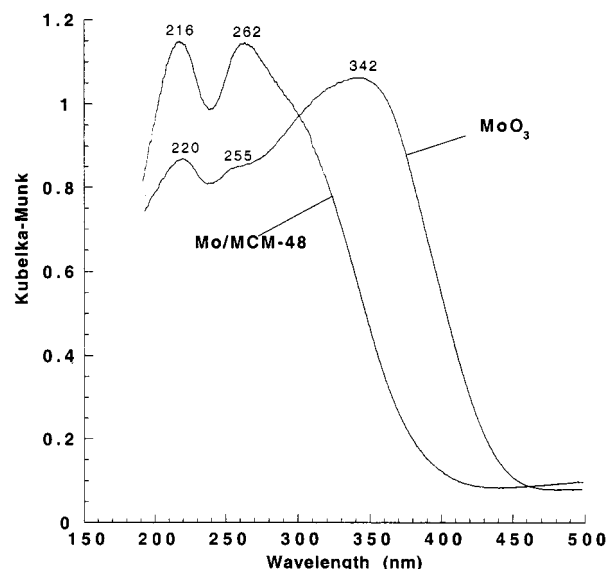
Ultraviolet/Visible Spectroscopy. Diffuse reflection UV/visible spectroscopy is a quick yet potent method for determining local molecular coordination sphere and bonding information for inorganic compounds such as simple mixed oxides. For fully oxidized, grafted metal ions, the predominant feature is the spin-allowed ligand to metal charge transfer (LMCT) from an O²⁻ ion t_{1u} orbital to a Mⁿ⁺ metal e_g orbital. Since each metal is in the d⁰ state, there are little or no d → d transitions observed, which are symmetry forbidden. Slight coloration in the resulting products can arise from incomplete surfactant oxidation during calcination or reduction of the metal center, as in the case of molybdenum. After the final stage of calcination, complete oxidation of metal centers can be verified by visual inspection for color: Ti, white; Mo and W, light beige to white; V, pale yellow; Zr and Re, white.

The surface species generated by grafting molybdenum using a number of different precursors has been thoroughly explored with UV/visible spectroscopy.^{16,19,26–29} Unfortunately, a general consensus remains elusive. The two primary difficulties in deciphering the UV/vis

Table 2. UV/Visible Spectra Results and Assignments from the Literature and This Work

sample	Mo source	peaks obsd (nm)	assgnt	ref
Mo/ZSM-5	(NH ₄) ₆ Mo ₇ O ₂₄	230 266	monomeric T _d polymeric O _h	26
Mo/SiO ₂	(NH ₄) ₂ Mo ₂ O ₇	230 270–280 sh	O _h , T _d T _d	27
Mo/SiO ₂	MoOCl ₄	305 230 280–295	polymeric O _h O _h or T _d O _h	28
Mo/SiO ₂	Mo ₂ (η ³ -C ₃ H ₅) ₄	290	monomeric T _d	29
Mo/MCM-48 (dry)	Mo ₂ (OC ₂ H ₅) ₁₀ ^a	216 262	O _h or T _d O _h	this work
W/MCM-48 (dry)	W(OC ₂ H ₅) ₅	216 264	O _h or T _d O _h	this work

^a Molybdenum precursor contains small impurity of MoO(OEt)₃.

**Figure 3.** Diffuse reflectance ultraviolet/visible spectra of Mo-grafted MCM-48 compared to crystalline molybdenum trioxide.

spectrum is the lack of significant peak data and the wide variety of metal precursors. For molybdenum(VI) on silica, the typical spectrum has between one and three peaks occurring between 240 and 300 nm. The results of the numerous studies on this system are assembled in Table 2. The main discrepancy arises from the assignment of the higher energy absorption as octahedrally or tetrahedrally coordinated molybdenum. If isolated, tetrahedrally coordinated molybdenum species are to be found on the silica surface, it is most likely in the samples prepared by grafting of water sensitive organomolybdate precursors. When amorphous silica was used, the surface silanol density was up to 3.5 OH/nm² allowing the possible formation of four-coordinate Mo ions consisting of 2 Mo–O–Si bonds and two terminal Mo=O bonds. Each of the above-mentioned studies made use of other analytical techniques to support their claims to different degrees.

When molybdenum is grafted on MCM-48, the UV/visible spectra have 3 predominant features (Figure 3). Two strong peaks are observed at 216 and 262 nm, with a shoulder at around 300 nm. A small dip occurs at about 310 nm when the spectrometer changes filters. Since the samples were run under ambient conditions,

(26) Cid, R.; Llambias, F. J. G.; Agudo, A. L.; Villasenor, J. J. *Catal.* **1984**, *89*, 478.

(27) Seyedmonir, S. R.; Howe, R. F. *J. Catal.* **1988**, *110*, 216.

(28) Plyuto, Y. V.; Babich, I. V.; Plyuto, I. V.; VanLangeveld, A. D.; Mouljn, J. A. *Colloids Surf. A* **1997**, *125*, 225.

(29) Iwasawa, Y.; Yamagishi, M. *J. Catal.* **1983**, *82*, 373.

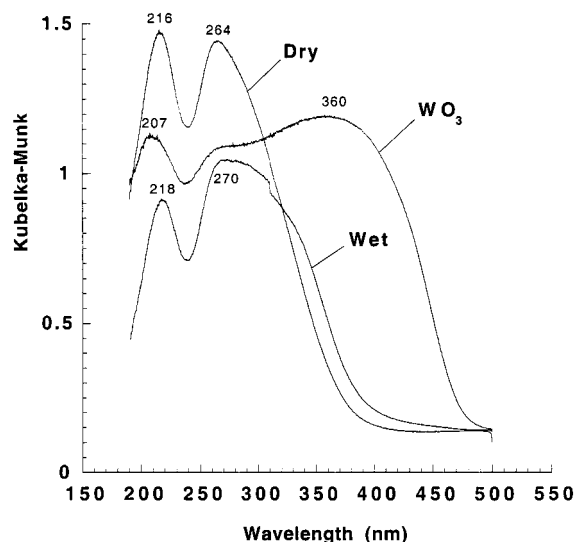


Figure 4. Diffuse reflectance ultraviolet/visible spectra of W-grafted MCM-48 run dry and wet as a paste with water. Pure, crystalline tungsten trioxide is used for comparison.

it is likely some water coordination occurred. The peaks at 262 and 300 nm can readily be assigned to isolated octahedral coordinated molybdenum ions and the beginnings of polymeric bulk molybdena, respectively. The peak at 216 nm will be tentatively assigned to isolated tetrahedral molybdenum species shifted to higher energies. This assignment is relatively risky based on a rather thorough study by Williams et al.³⁰ In their Raman spectroscopy study, molybdenum was supported on silica using a variety of Mo precursors (excluding $\text{Mo}_2(\text{OC}_2\text{H}_5)_{10}$) yielding no detectable isolated Mo-oxy tetrahedra, as determined by the absence of the Raman active tetrahedral normal mode. They also found that different species arise upon hydration of the samples. Some of our Mo-containing samples had a faint blue color indicating the presence of Mo(V) species. Since the sample of Mo/MCM-48 "burned" when exposed to the Raman laser even at the lowest power, this method could not be used to confirm the assignment of the peak at 216 nm. For future reference, the sample can be rapidly spun to avoid the localized heating problem caused by the laser.³¹

A more convincing argument for the assignment of the high-energy peak to an isolated tetrahedral environment can be seen in the UV/visible spectra for tungsten grafted by the same method (Figure 4). In this case, a 7.4 at. % W sample (XS-W) was analyzed "as received" and mixed with water to form a paste. Peak assignments are the same as for the Mo-containing sample since the similar chemistries of the two elements are well-known. A noticeable change in the relative peak intensities between the two main peaks is observed when the sample is mixed with water. To begin with, both peaks shift to lower energies upon introduction of moisture. Then, the intensity of the peak corresponding to octahedral molybdenum (260–270 nm) increases at the expense of the intensity of the higher energy peak. The interrelation of these two peaks could be most easily

interpreted as a tetrahedrally coordinated W (or Mo) atom increasing its coordination sphere to six with the addition of two water ligands. In both cases, each sample is relatively free of bulk metal oxide down to the detection level for this technique illustrated by the blue-shifted cutoff wavelength of the absorption bands versus those for the various pure metal oxides.

Photoacoustic-FTIR of Grafted Metal Ions. Photoacoustic (PAS)-FTIR has proven itself to be a powerful technique in determining the degree of interaction between grafted metal ions and their mesoporous supports. The spectrum of the pure silica MCM-48 support (Figure 5b) can be divided into two separate regions, surface and framework. In the higher energy portion of the spectrum is the O–H stretch of the surface silanols. Isolated silanols, which have no hydrogen-bonding effects, give rise to a sharp peak at 3745 cm^{-1} . Adjacent silanols as well as the O–H stretch of physisorbed water are shifted to a lower frequency and are more readily resolved with diffuse reflectance FTIR (spectra not shown). Closely related to the O–H peak for surface silanols is another sharp peak for the $\text{Si}^{\delta+}\text{O}^{\delta-}$ stretch of the silanol group at 978 cm^{-1} .

Primary infrared absorption bands related to the silica framework occur from 1400 to 400 cm^{-1} with overtones from 2100 to 1800 cm^{-1} . The bending of physisorbed water occurs around 1615 cm^{-1} . The predominant series of peaks from 1300 to 980 cm^{-1} correspond to the asymmetric stretch (ν_{as}) of the Si–O–Si bond. For samples of mesoporous materials made with the two-step hydrothermal treatment, the three IR-active bands associated with this vibration can be partially resolved, at 1243 , 1180 , and 1083 cm^{-1} , respectively. The most significant of these peaks is the sharp 1243 cm^{-1} absorption which is reported to result from ordered chains of silicate "five-rings" in zeolitic systems.³² The existence and resolution of this peak is a preliminary but convincing argument for a degree of intermediate range order within the silicate walls. Further evidence of this assertion is seen by the presence of a broad peak at 600 cm^{-1} which is not found in the FTIR spectrum of amorphous silica, setting it apart from all other forms of crystalline silicates. The peak at 600 cm^{-1} is referred to as the "crystallinity peak" in zeolite studies as it is used as a preliminary criteria for the formation of ordered, network solids.^{33–35} On the basis of the sharpness of the peaks at 3745 , 1243 , and 978 cm^{-1} , we speculate that they are related in that the framework band at 1243 cm^{-1} could be associated with an isolated silanol group.³⁶ The remaining peaks at 817 and 460 cm^{-1} are assigned to the symmetric stretch (ν_{s}) of the Si–O–Si bond and the Si–O bending vibration, respectively.

The primary purpose of the grafting technique for loading silica surfaces with transition metal ions is to ideally generate isolated metal ions directly bonded to the support through Si–O–M covalent bonds. The presence of isolated metal ions on the surface is favored

(30) Williams, C. C.; Ekerdt, J. G.; Jehng, J.-M.; Harcastle, F. D.; Turek, A. M.; Wachs, I. E. *J. Phys. Chem.* **1991**, *95*, 8781.

(31) Strommen, D.; Nakamoto, K. *Laboratory Raman Spectroscopy*; Wiley: New York, 1984.

(32) Jansen, J. C.; Van der Gaag, F. J.; Van Bekkum, H. *Zeolites* **1984**, *4*, 369.

(33) Flanigen, E. M.; Khatami, H.; Szymanski, H. A. *Adv. Chem. Ser.* **1971**, *101*, 201.

(34) Coudurier, G.; Naccache, C.; Vadrine, J. C. *J. Chem. Soc., Chem. Commun.* **1982**, 1413.

(35) Jacobs, P. A.; Beyer, H. K.; Valyon, J. *Zeolites* **1981**, *1*, 161.

(36) Flanigen, E. Personal communication.

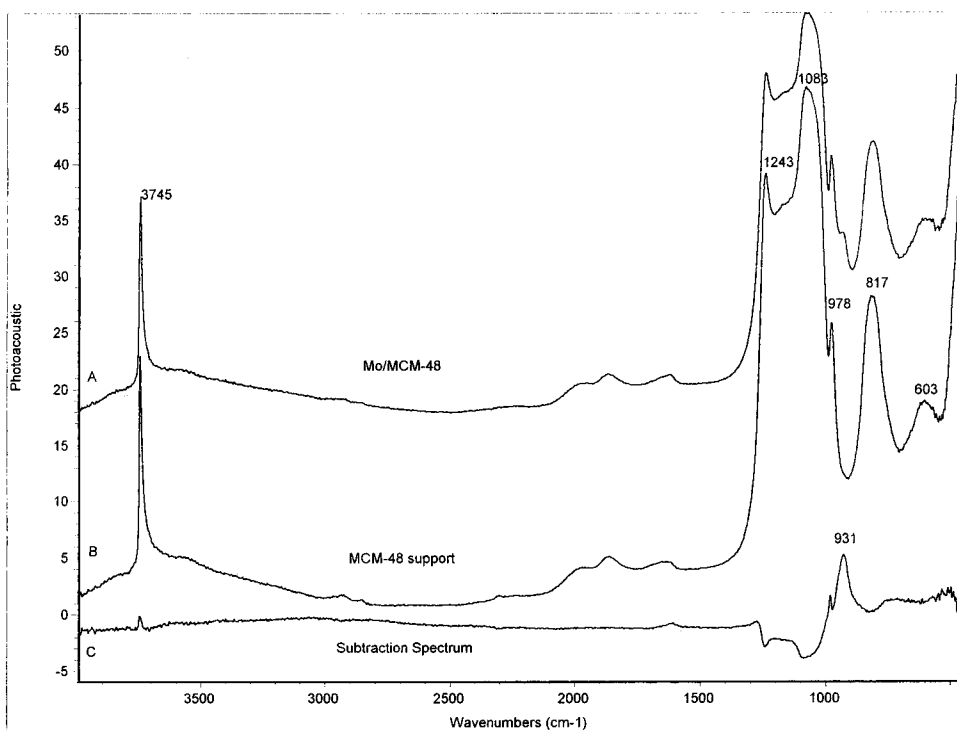
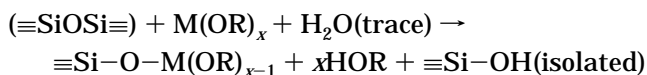


Figure 5. PAS-FTIR of (a) Mo/MCM-48, (b) pure silica MCM-48, and (c) the subtraction result.

in the grafting reaction if care is taken to avoid water. Metal alkoxides tend to form dimers in solution, leading to a "molecular complexity" of greater than one. The molybdenum ethoxide precursor is actually dimolybdenum decaethoxide with some $\text{MoO}(\text{OEt})_3$ while tungsten (V) ethoxide is supposed to be monomeric. The point here is that if the precursor is dimeric in solution with hexane, neighboring metal ions could be laid down on the surface.

To determine the degree of metal ion interaction with the silica surface, changes in the PAS-FTIR spectra of both the silanol and framework regions were observed. An initial grafting blank spectrum showed no change in absorbances in either the silanol or framework regions after treatment with just hexane. As with UV/visible spectroscopy, numerous FTIR studies have been conducted on molybdenum/silica systems, except with an uncharacteristic degree of agreement concerning band assignments. In Figure 5, the subtraction spectra of 3 at. % Mo on MCM-48 is given. There is a net increase in the isolated silanol peak at 3745 cm^{-1} after grafting which is unexpected, on the basis of the extensive previous results with Ti and V grafted samples.⁸ A possible scenario is the attack of Mo on a nearby strained Si–O–Si bridge or a hydrogen-bound silanol to generate a Mo–O–Si bridge and an additional isolated silanol:



In the framework region of the subtraction spectrum, a new and distinct peak is seen at 931 cm^{-1} which is assigned to a Mo–O–Si stretch. The peak position can be explained as a shift to lower wavenumbers of the (ν_{as}) Si–O–Si frequency when one silica is replaced with a heavier atom, in accordance with a simple harmonic

oscillator model. This band has been reported for silica-supported samples made from a number of different molybdenum precursors.^{27,37,38} The presence of this band is a clear indication of the strong interaction between the molybdenum ions and the silica surface.

Adding credence to the concept of periodicity, grafted tungsten exhibits the same trends in bonding with the surface of MCM-48. When a stoichiometric excess of W is grafted (corresponding to 7.4 mol % W), similar changes in the FTIR spectrum are seen when compared to Mo. In the subtraction spectrum Figure 6, a net gain in isolated silanol groups is noted. In the framework region, two additional peaks are seen at 921 and 739 cm^{-1} which are tentatively assigned to W–O–Si and edge-sharing W–O–W bonds.⁵⁷ On the basis of the sparse infrared studies of silica supported tungstates, the assignment of the 921 cm^{-1} peak to a W–O–Si bond is more appropriate than a higher energy W=O bond. A smaller shoulder at about 855 cm^{-1} could be attributed to the formation of dodecatungstosilicic acid units on the surface.³⁹ It is likely that, at lower loadings, the W–O–W peak would disappear as tungsten ions become more distant from each other. In Figure 7, the framework region of the subtraction spectra for a number of different transition metals grafted on MCM-48 is shown. It is clear that since the M–O–Si stretching frequency does not strictly follow a reduced mass spring constant argument, other interatomic forces must play a roll in this value. The resulting frequencies for the M–O–Si bonds are listed in Table 3 by order of atomic weight.

(37) Seyedmonir, S. R.; Abdo, S.; Howe, R. F. *J. Phys. Chem.* **1982**, *86*, 1233.

(38) El Shafei, G. M. S.; Mokhtar, M. *Colloids Surf. A* **1995**, *94*, 267.

(39) Martin, C.; Malet, P.; Solana, G.; Rives, V. *J. Phys. Chem. B* **1998**, *102*, 2759.

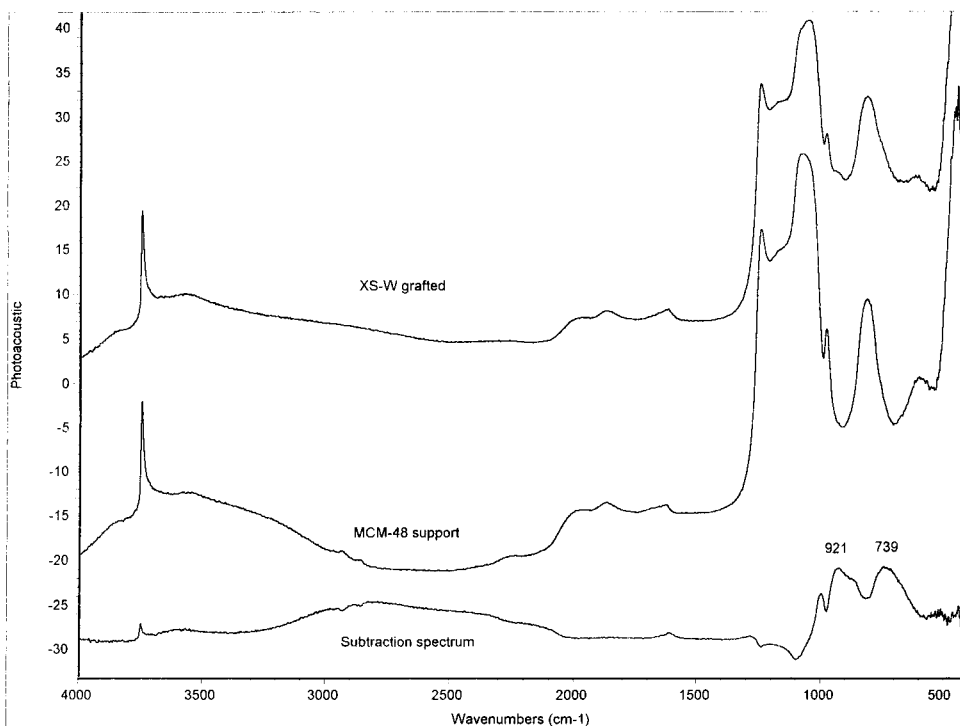


Figure 6. PAS-FTIR of (a) W/MCM-48, (b) pure silica MCM-48, and (c) the subtraction result.

Table 3. M–O–Si Asymmetric Stretches (cm⁻¹) for Grafted Metal Species Determined by PAS-FTIR

	Ti	V	Zr	Mo	W ^a	Re ^a
M–O–Si (ν_{as})	931	924	942	931	921	945

^a Tentatively assigned.

Metal–Peroxo Intermediates and Relative Reactivities

We have found that grafted titanium on MCM-48 catalyzes the peroxidative halogenation of large organic substrates such as phenol red.⁹ Despite their size, it is necessary for the phenol red molecules to percolate into the pore system for bromination to occur. In the absence of a nearby substrate, the oxidized bromine species will oxidize a second equivalent of H₂O₂ to form singlet oxygen.¹⁰ In addition to titanium, the five other transition metals listed above were tested in the same fashion and found to react at different rates.⁴⁰ The relative reactivity rate was determined by measuring the visible absorbance of the bromophenol product after a fixed amount of time for each of the grafted metals. The rates were then compared after normalization on the basis of the metal concentrations from elemental analysis and the assumption of a linear dependence of rate on metal atom surface density, at these relatively low metal loadings. When the extents of the reactions were expressed as a relative ratio of absorption values at 589 nm after 60 min, the six grafted transition metals catalyzed the bromination of phenol red in the following order: 50:46:16:2.8:1:0 W:Mo:Ti:Zr:V:Re. There is no lack of irony in the fact that grafted vanadium is practically inactive for halogenation, since the original vanadium-containing enzyme that initiated this catalytic study, V–BrPO, is so effective at this task.¹⁰ When

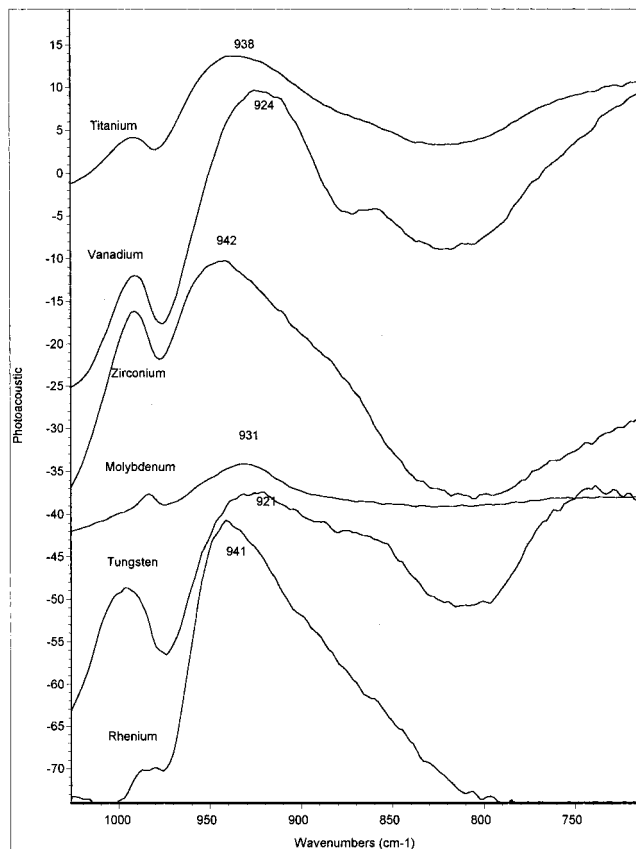


Figure 7. Expanded framework region of various transition metals grafted on MCM-48 generated by subtracting the pure silica MCM-48 vibrations from the metal-grafted spectrum. (Note: The "peak" at 995 cm⁻¹ is an artifact of subtraction while the dip at 978 cm⁻¹ reflects a spectral decrease in the silanol vibration after grafting.)

the supernatant was tested, some brominating activity was observed with a solution of Na₂WO₄(aq) and pure silica MCM-48 but was much slower than the grafted

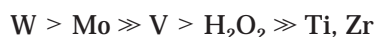
(40) Morey, M. S.; Walker, J. V.; Carlsson, H.; Davidson, A.; Butler, A.; Stucky, G. D. To be submitted for publication.

sample or the analogous $\text{MoO}_4^{2-}(\text{aq})$ case. To have a significant degree of bromination occur, the homogeneous reactions need to be run under acidic conditions (0.1 M HClO_4).¹⁰

Beyond different reactivities toward peroxidative halogenation, the larger question that must be asked is what are the trends that govern transition metal activation of hydrogen peroxide in its plethora of catalytic applications? In our case, six transition metals were tested for the same reaction with quite different results. Rhenium, zirconium, and vanadium were all found to be more or less inactive. Titanium was active for halogenation, which was noteworthy, since there are no titanium containing biomimics known. This activity is not unexpected due to its widespread success as an industrial oxidation catalyst. Tungsten and molybdenum were found to be about twice as active as titanium, with tungsten being the fastest by a small margin. Since the only variable in the test is the choice of transition metal, the reasonable place to explore is the nature of each metal and its interaction with the peroxide ligand(s) on the intermediate. The study of the nature of the transition metal can be split into interrelated, local atomic properties such as ionic radius, formal charge, electronegativity, and coordination number, with accompanying periodicity arguments. In a proposed metal-peroxo intermediate, the effect of these properties on the strength of the O–O bond of the peroxo ligand as well as the Brønsted acidity of the hydrogen will be discussed.

In the literature, numerous d^0 metal oxo peroxo complexes have been studied to determine the relationship among their structures, spectroscopic properties, and relative abilities to activate the peroxide ligand. This difficult problem is compounded by the number of different complexes possible for each metal and the fact that different mechanisms for the oxidation process may be involved. Determining the structure/reactivity relationship for aqueous species will give insight into the relative reactivity of the silica supported metals. In solution, the majority of M-peroxo complexes have the peroxo group bound "side-on", as determined from single-crystal X-ray diffraction of their salts.^{14,41,42} Few exceptions do exist such as $[\text{MoO}(\text{O}_2)_2(\text{OOH})]_2^{2-}$.¹⁴ The early transition metals readily coordinate peroxide ligands from solution at a rate which increases with acid concentration.^{43,44} The number of peroxide ligands surrounding each metal center ranges from 0.5 for $\text{Zr}_4(\text{O}_2)_2(\text{OH})_4^{8+}$,⁴⁴ one to two for titanium, $\text{Ti}(\text{O}_2)(\text{OH})^+$, and vanadium, $\text{VO}(\text{O}_2)_2^-$, and up to four for molybdenum and tungsten, $\text{W}(\text{O}_2)_4^{2-}$.^{14,45} As a side note, much Raman data of the tetraperoxy species are missing because the compounds tend to explode.¹⁴ Vanadium, molybdenum, and tungsten also form oxo-peroxo and oxo-diperoxo $\text{MO}(\text{O}_2)_2(\text{H}_2\text{O})_2$ species as well. Their structures consist of the peroxo ligands bound side on in a plane perpendicular to the terminal M=O bond with σ -interaction between the metal d_{xy} orbital and the peroxo π^* orbital.⁴⁵

Once the metal peroxo complex is formed, it becomes an effective oxidant in solution, often orders of magnitude better than unbound hydrogen peroxide.⁴⁶ Many studies have compared the reactivity of different metal peroxide complexes with respect to the types of ligands and the choice of metal center and have observed some interesting and consistent trends. Schwane et al. showed that the coordinated peroxo ligand is activated in $\text{MoO}(\text{O}_2)_2(\text{OH})^-$ and $\text{WO}(\text{O}_2)_2(\text{OH})^-$ but not for $\text{Ti}(\text{O}_2)(\text{OH})^+$.⁴³ They proposed that the oxo-peroxo ligand combination plays an important role in the activation process. This observation can account for any activity contribution from aqueous species resulting from the slow hydrolysis of the M–O–Si bond for grafted metal ions on MCM-48. When there is comparison with vanadium and zirconium peroxo species as well as free peroxide, Ghiron et al.⁴⁶ states that their relative oxidative abilities have the following order in solution:



For epoxidation and sulfide oxidation, $\text{WO}(\text{O}_2)_2(\text{hmp})$ has a greater catalytic efficiency than its molybdenum analogue.¹⁴ This order was confirmed in the oxidation of bromide ions by aqueous metal peroxo species in acidic solution as biomimics of the vanadium bromoperoxidase enzyme.¹² For the case of an ideal heterogeneous catalyst, any aqueous leachates must be inert.^{58,59}

Many attempts have been made to study metal peroxo complexes by X-ray diffraction, FTIR, NMR, and cyclic voltammetry to correlate reactivity trends with intrinsic molecular properties and structure. Single crystals of metal peroxo salts can be easily isolated and analyzed by the above techniques. X-ray diffraction yields useful information about the O–O bond length and the overall coordination sphere of the central metal ion. For the metal oxo peroxo series of V, Mo, and W, the O–O bond length increases from 1.46 to 1.51 Å indicating a longer and thus weaker O–O bond for the tungsten species. This weakening of the O–O bond follows the general reactivity order as given above.⁴⁶ Furthermore, in the order from a monoperoxo to a diperoxo, the O–O bond length increases from 1.43 to 1.47 Å.

FTIR spectroscopy has been used extensively to measure the O–O vibration of bound peroxide species. Occurring in the range from 940 to 750 cm^{-1} , the $\nu(\text{O}–\text{O})$ stretch is highly affected by its host. The oxyhemocyanin enzyme, which is a dioxygen carrier for mollusks, possesses a Cu-peroxo group with an abnormally low $\nu(\text{O}–\text{O})$ of 750 cm^{-1} .⁴⁷ For different groups in the early transition metals such as V, Nb, Ta and Cr, Mo, W, there is a consistent decrease in the $\nu(\text{O}–\text{O})$ frequency with increased atomic weight of the metal.^{41,46,48–50} This trend among metal peroxo complexes was found for both constant metal or constant ligand, $(\text{O}_2)\text{ML} \rightarrow (\text{O}_2)\text{ML}'$ or $(\text{O}_2)\text{ML} \rightarrow (\text{O}_2)\text{M}'\text{L}$. It is also seen for monoperoxo to diperoxo, as 2 ligands compete for the metal and decrease their bonding

(46) Ghiron, A. F.; Thompson, R. C. *Inorg. Chem.* **1990**, *29*, 4457.

(47) Moro-Oka, Y.; Fujisawa, K.; Kitajima, N. *Pure Appl. Chem.* **1995**, *67*, 241.

(48) Gresley, N. M.; Griffith, W. P.; Laemmel, A. C.; Nogueira, H. I. S.; Parkin, B. C. *J. Mol. Catal. A: Chem.* **1997**, *55*, 185.

(49) Dengel, A. C.; Griffith, W. P. *Polyhedron* **1989**, *8*, 1371.

(50) Campbell, N.; Dengel, A. C.; Griffith, W. P. *Polyhedron* **1989**, *8*, 1379.

(41) Campbell, N. J.; Bengel, A. C.; Edwards, C. J.; Griffith, W. P. *J. Chem. Soc., Dalton Trans.* **1989**, 1203.

(42) Gubelmann, M. H.; Williams, A. F. *Struct. Bond.* **1984**, *55*, 2.

(43) Schwane, L. M.; Thompson, R. C. *Inorg. Chem.* **1989**, *28*, 3938.

(44) Thompson, R. C. *Inorg. Chem.* **1985**, *24*, 3542.

(45) Reynolds, M. S.; Butler, A. *Inorg. Chem.* **1996**, *35*, 2378.

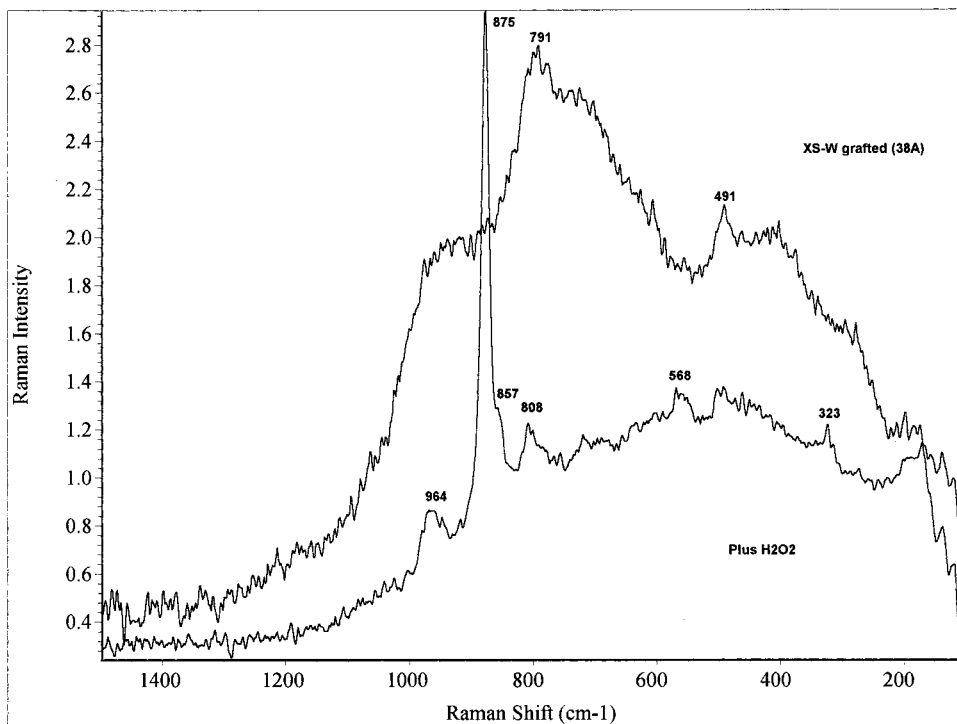


Figure 8. Raman spectra of tungsten-grafted MCM-48 run dry and as a slurry with 1% aqueous hydrogen peroxide.

interaction with the central metal.⁴⁵ Bonchio et al. used cyclic voltammetry to study a number of metal peroxo complexes and found the reduction potentials increased in parallel with the O–O bond strength.⁵¹

The PAS-FTIR spectra of Ti grafted on MCM-48 and then treated with H₂O₂ show a new peak at 886 cm⁻¹, which is attributed to the $\nu(\text{O}-\text{O})$ stretch of a stable, bound Ti–peroxo intermediate. The corresponding weakening of this O–O bond is quite substantial and comparable with aqueous, monoperoxo complexes of Mo, V, Cr, and W.^{45,52} This is in contrast to zirconium and rhenium for which there was no catalytic activity or evidence of peroxide complexation. Molybdenum and tungsten catalyzed the decomposition of H₂O₂ too rapidly to unambiguously identify a metal–peroxo intermediate. However, Raman spectroscopy on a Mo,W/MCM-48, $\approx 1\%$ H₂O₂ slurry resulted in new peaks to the right of free peroxide (875 cm⁻¹) at 857 and 808 cm⁻¹ which are consistent with $\nu(\text{O}-\text{O})$ stretches of two types of complexed metal–peroxo intermediates.⁵⁷ The presence of an aqueous phase was helpful though in preventing burning of the samples (Figure 8).

The above results are interrelated and can be satisfactorily explained in terms of electronegativity and the effect ligand electron withdrawing has on the O–O bond. In Figure 9, a number of proposed metal peroxo intermediates and peroxide activation pathways are presented. In each, the O–O bond of the bound peroxide group is polarized by the electron-withdrawing effects of the central metal. The bond polarity then promotes heterolytic O–O bond cleavage upon nucleophilic attack, favoring a nonradical pathway for oxidative bromination via a reactive OBr⁻ species, as seen for molybdenum.¹²

Polarization of the O–O bond is also seen in titanium silicalite-1, where electrons are withdrawn by the strongly acidic Lewis center ($-\text{Ti}(-\text{OSiO}_3)_3$).⁵³ Since it is agreed that the rate-limiting step for oxygen transfer is the cleavage of the O–O bond, the longer and thus weaker O–O bonds are found on the most active compounds.^{45,46} This effect is enhanced by a number of different factors. As stated above, if more than one peroxide ligand is bound, the O–O bond strength decreases as a maximum mixing between d orbitals and peroxide orbitals yields an increased antibonding character in the O–O bond.^{45,46} For metals in the fourth and fifth row of the d block, the distance between the electron density lobes of the d orbitals and the nucleus increases. This increase causes the 5d orbitals on tungsten to overlap more with the peroxide ligand orbitals and increases the antibonding character of the O–O bond thus facilitating its cleavage. The presence of an electron-withdrawing M=O bond, predominantly in Mo and W complexes, further acts to draw additional electron density from the O–O bond.⁴⁷

The activity of early transition metal peroxo complexes is also proportional to their Lewis acidity,⁵⁴ which in turn is dependent on the electronegativity of the metal. The electronegativities for each metal studied are given in Table 4. In their fully oxidized states, hexavalent tungsten followed by molybdenum clearly is the most Lewis acidic and electrophilic within the series of interest. On the basis of the electron-withdrawing effects of the ligands and central metal on the O–O bond of the peroxide ligand, it is therefore not surprising that

(53) Clerici, M. G.; Ingallina, P. *J. Catal.* **1993**, *140*, 71.

(54) Ghiron, A. F.; Thompson, R. C. *Inorg. Chem.* **1989**, *27*, 4766.

(55) Allred, A. L. *J. Inorg. Nucl. Chem.* **1961**, *17*, 215.

(56) Margolese, D. Dissertation, UCSB Chemistry Department, 1995.

(57) Orel, B.; Opara Krašovec, U.; Grošelj, N.; Kosec, M.; Dražič, G.; Reisfeld, R. *J. Sol-Gel Sci. Technol.* **1999**, *14*, 291.

(51) Bonchio, M.; Conte, V.; DiFuria, F.; Modena, G.; Moro, S.; Carofiglio, T.; Magno, F.; Pastore, P. *Inorg. Chem.* **1993**, *32*, 5797.

(52) Reynolds, M. S.; Babinski, K. J.; Bouteneff, M. C.; Brown, J. L.; Campbell, R. E.; Cowan, M. A.; Durwin, M. R.; Foss, T.; O'Brien, P.; Penn, H. R. *Inorg. Chem. Acta* **1997**, *263*, 225.

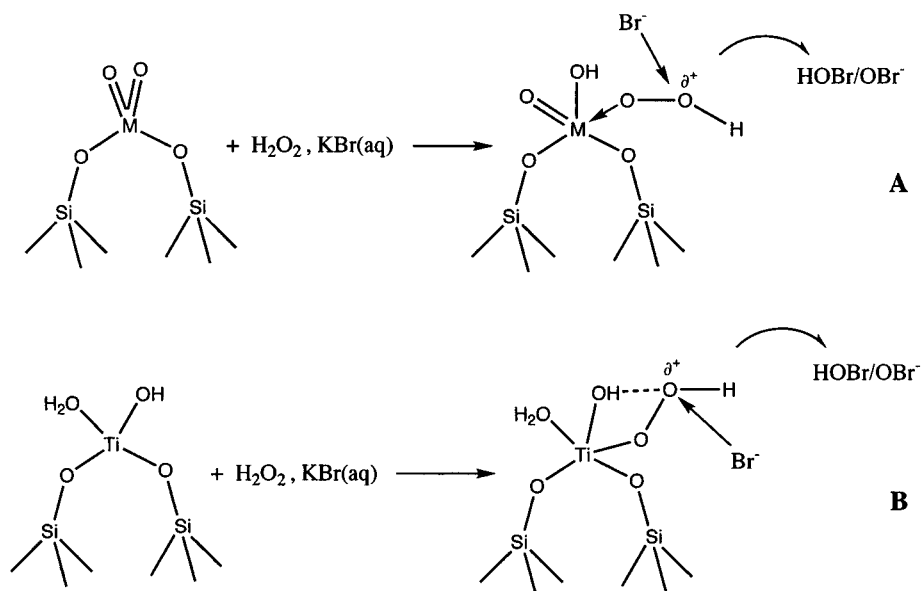


Figure 9. Possible configurations and mechanisms for O–O bond polarization of a coordinated peroxide molecule to a grafted metal center where M = Mo and W. Subsequent nucleophilic attack by bromide occurs to form a reactive intermediate for bromination of phenol red substrate.

Table 4. Formal Charge and Pauling Electronegativities for Early Transition Metals⁵⁵

	Ti	V	Zr	Mo	W
oxidation state	4+	5+	4+	6+	6+
electronegativity	1.5	1.6	1.4	1.8	1.7

tungsten and molybdenum supported on MCM-48 or in solution, in the presence of hydrogen peroxide, are the most effective oxidation catalysts in the series. Their improved activity over grafted titanium could further be enhanced by the fact that $\text{Ti}(\text{O}_2)(\text{OH})^+(\text{aq})$ is inert⁵⁸ while aqueous Mo, W oxo–peroxo species can still activate peroxide for bromination to some degree.

Conclusions

We have functionalized the surface of MCM-48 mesoporous silica with a number of early transition metals and rated their activity toward the bromination of a large organic substrate. By using reactive metal alkoxide precursors under anhydrous conditions, isolated metal species were grafted to the silica surface via M–O–Si bonds. By preferential generation of monomeric versus polymeric metal oxo species on the surface,

the study of the relationship between structure and reactivity is simplified. As with titanium, both molybdenum and tungsten are active at neutral pH, analogous to the conditions under which the vanadium bromoperoxidase enzyme functions.

On the basis of these observations, results, and theories, the predictive power concerning the potential activity of new catalysts has been broadened. As seen for the enzyme vanadium bromoperoxidase, which is orders of magnitude more active for peroxidative halogenation than the best biomimics, there is clearly room for improvement in this field. One approach could be to imitate the coordination sphere of the active metal site within an enzyme by binding carefully selected ligands, for example. Using the above guidelines, it should then be possible to develop more efficient and specialized transition metal-based catalysts, thus narrowing the gap between nature and innovation.

Acknowledgment. We gratefully acknowledge the NSF for funding under Award No. DMR-9520971. This work made use of the MRL Central Facilities supported by the National Science Foundation under Award No. DMR96-32716. M.S.M. wishes to thank Dr. Wayne Lukens and Professor A. Butler for thoughtful discussion and Håkan Carlsson for catalyst testing.

(58) Sheldon, R. A.; Wallau, M.; Arends, I. W. C. E.; Schuchardt, U. *Acc. Chem. Res.* **1998**, *31*, 485.

(59) Chen, L. Y.; Chuah, G. K.; Jaenicke, S. *Catal. Lett.* **1998**, *50*, 107.

(60) Lydon, J. D.; Thompson, R. C. *Inorg. Chem.* **1986**, *25*, 3694.